

## Cationic $\sigma$ -Phenylplatinum(II) Complexes with Carboxylic Acid Functionality: $pK_a$ Determinations and X-ray Structures

Michael G. Crisp, Edward R. T. Tiekink,<sup>†</sup> and Louis M. Rendina\*

Department of Chemistry, The University of Adelaide, Adelaide, South Australia 5005, Australia

Received June 7, 2002

The preparation and characterization of a novel series of cationic  $\sigma$ -phenylplatinum(II) complexes of the type *trans*-[Pt( $\sigma$ -C<sub>6</sub>H<sub>5</sub>)(L)<sub>2</sub>A]OTf (A = picolinic acid, L = PPh<sub>3</sub> (**4**) and PMePh<sub>2</sub> (**7**); A = nicotinic acid, L = PPh<sub>3</sub> (**5**) and PMePh<sub>2</sub> (**8**); A = isonicotinic acid, L = PPh<sub>3</sub> (**6**), PMePh<sub>2</sub> (**9**), and PEt<sub>3</sub> (**10**)) are described. The  $pK_a$  value for the carboxylic acid functionality in selected complexes was found to follow the order **7** ( $pK_a = 5.23 \pm 0.09$ ) > **8** ( $4.85 \pm 0.10$ ) > **9** ( $3.51 \pm 0.08$ ) > **6** ( $3.26 \pm 0.07$ )  $\approx$  **10** ( $3.21 \pm 0.08$ ) by means of potentiometric titration experiments in 50% (v/v) EtOH/H<sub>2</sub>O solution at 295 K. The X-ray crystal structures of **9** and **10** were also determined. The asymmetric unit of each of **9** and **10** comprises a univalent complex cation, a triflate anion, and a solvent CH<sub>2</sub>Cl<sub>2</sub> molecule of crystallization. Centrosymmetrically related pairs of complex cations in **9** associate via the familiar carboxylic acid dimer motif, whereas with **10**, the carboxylic acid dimer motif is absent. Instead, the carboxylic acid residue forms both donor and acceptor interactions to the triflate anion and CH<sub>2</sub>Cl<sub>2</sub> solvent of crystallization, respectively, to afford a 10-membered ring structure. Possible reasons for the observed differences in the solid-state structures of **9** and **10** are presented.

### Introduction

Major advances have been made in the use of the coordinate-covalent bond for the construction of large molecular polygons and polyhedra by self-assembly.<sup>1</sup> More recently, the combination of the coordinate-covalent and H-bonding motifs has been shown to expand the utility of metal complexes as tectons<sup>2</sup> (building blocks) in the con-

struction of large molecular polygons and other types of supramolecular arrays,<sup>3</sup> particularly when the H-bonding interactions are enhanced via charge-assistance by the use of ionic complexes.<sup>3a</sup> Diverse examples of the simultaneous use of these bonding motifs in late-transition-metal chemistry include the synthesis of a unique organoplatinum(IV) polyrotaxane with a remarkable architecture,<sup>4</sup> the assembly of infinite single- and double-stranded chains by isonicotinamide complexes of platinum(II) and rhodium(III),<sup>5</sup> respectively, a cyclic tetramer of platinum(II) complexes containing 5-aminoorotic acid,<sup>6</sup> the self-assembly of sheet and polymer structures by pyridine-carboxamide complexes of palladium(II),<sup>7</sup> infinite 1D-, 2D-, and 3D-assemblies involving silver(I) complexes of nicotinamide and isonicotinamide,<sup>8</sup> and the

\* To whom correspondence should be addressed. E-mail: lou.rendina@adelaide.edu.au. Phone: 61 8 8303 4269. Fax: 61 8 8303 4358.

<sup>†</sup> Present address: Department of Chemistry, National University of Singapore, Singapore 117543.

(1) For recent reviews, see: (a) Olenyuk, B.; Fechtenkötter, A.; Stang, P. *J. J. Chem. Soc., Dalton Trans.* **1998**, 1707. (b) Fujita, M.; Ogura, K. *Coord. Chem. Rev.* **1996**, *148*, 249. (c) Fujita, M. *Chem. Soc. Rev.* **1998**, *27*, 417. (d) Stang, P. J.; Olenyuk, B. *Acc. Chem. Res.* **1997**, *30*, 502. (e) Jones, C. J. *Chem. Soc. Rev.* **1998**, *27*, 289. (f) Stang, P. J. *Chem. Eur. J.* **1998**, *4*, 19. (g) Baxter, P. N. W. In *Comprehensive Supramolecular Chemistry*; Lehn, J.-M., Chair, E., Atwood, J. L., Davies, J. E. D., MacNicol, D. D., Vögtle, F., Eds.; Pergamon Press: Oxford, 1996; Vol. 9, p 165. (h) Caulder, D. L.; Raymond, K. N. *J. Chem. Soc., Dalton Trans.* **1999**, 1185. (i) Caulder, D. L.; Raymond, K. N. *Acc. Chem. Res.* **1999**, *32*, 975. (j) Chambron, J.-C.; Dietrich-Buchecker, C.; Sauvage, J.-P. In *Comprehensive Supramolecular Chemistry*; Lehn, J.-M., Chair, E., Atwood, J. L., Davies, J. E. D., MacNicol, D. D., Vögtle, F., Eds.; Pergamon Press: Oxford, 1996; Vol. 9, p 43. (k) Ullert, E.; Demleitner, I.; Bernt, I.; Saalfrank, R. W. In *Structure and Bonding*; Fujita, M., Ed.; Springer: Berlin, 2000; Vol. 96, p 149. (l) Leininger, S.; Olenyuk, B.; Stang, P. *J. Chem. Rev.* **2000**, *100*, 853. (m) Halpern, J. *Proc. Natl. Acad. Sci. U.S.A.* **2002**, *99*, 4762 and references therein.

(2) Simard, M.; Su, D.; Wuest, J. D. *J. Am. Chem. Soc.* **1991**, *113*, 4696.  
(3) For recent reviews, see: (a) Braga, D.; Grepioni, F. *Acc. Chem. Res.* **2000**, *33*, 601. (b) Braga, D.; Grepioni, F.; Desiraju, G. R. *Chem. Rev.* **1998**, *98*, 1375. (c) Aakeröy, C. B.; Beatty, A. M. *Aust. J. Chem.* **2001**, *54*, 409. (d) Burrows, A. D.; Chan, C.-W.; Chowdhry, M. M.; McGrady, J. E.; Mingos, D. M. P. *Chem. Soc. Rev.* **1995**, 329.  
(4) Fraser, C. S. A.; Jennings, M. C.; Puddephatt, R. J. *Chem. Commun.* **2001**, 1310.  
(5) Kuehl, C. J.; Tabellion, F. M.; Arif, A. M.; Stang, P. J. *Organometallics* **2001**, *20*, 1956.  
(6) Burrows, A. D.; Mingos, D. M. P.; White, A. J. P.; Williams, D. J. *J. Chem. Soc., Dalton Trans.* **1996**, 3805.  
(7) Qin, Z.; Jennings, M. C.; Puddephatt, R. J. *Inorg. Chem.* **2001**, *40*, 6220.

construction of nanoscale cyclic arrays containing platinum(II) and nicotinic acid.<sup>9</sup>

Herein we describe the synthesis and characterization of a series of  $\sigma$ -phenylplatinum(II) complexes with a carboxylic acid functionality incorporated through the use of pyridine monocarboxylic acid ligands. The ability of these model compounds to act as tectons both in solution and in the solid state is limited by the presence of only one carboxylic acid functionality, but despite this limitation, their association in the solid state is found to differ quite remarkably. The  $\sigma$ -phenyl ligand simply serves to block one of the coordination sites in these model complexes, and it may also participate in favorable  $\pi$ - $\pi$  stacking interactions. We also report the  $pK_a$  values for a selected number of complexes in order to determine the effect of platinum coordination on the Brønsted acidity of the free CO<sub>2</sub>H group, the results of which have particular relevance to studies of molecular recognition involving these and related species in solution, particularly in polar solvent systems.

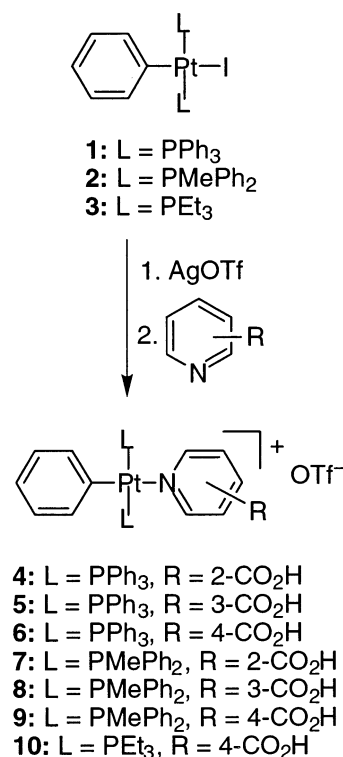
### Synthesis and Characterization of $\sigma$ -Phenylplatinum(II) Complexes with Carboxylic Acid Functionality

The target  $\sigma$ -phenylplatinum(II) complexes were prepared from the corresponding iodo complexes **1–3** by treatment with 1 equiv of AgOTf in CH<sub>2</sub>Cl<sub>2</sub> solution to afford the labile  $\sigma$ -phenyl(triflate)platinum(II) species. The addition of isomeric pyridine monocarboxylic acids (picolinic acid, nicotinic acid, and isonicotinic acid) readily afforded the target cationic complexes **4–10** as air-stable, microcrystalline solids in good yield and purity (Scheme 1). The products were fully characterized by 1D (<sup>1</sup>H, <sup>31</sup>P, and <sup>19</sup>F)- and 2D (<sup>1</sup>H-<sup>1</sup>H COSY) NMR and IR spectroscopy, microanalysis, and, in the case of **9** and **10**, by X-ray crystallography.

The <sup>1</sup>H NMR spectrum of **5** shows multiplet signals at  $\delta$  6.74, 6.37, and 6.53, which correspond to the *ortho*, *meta*, and *para*  $\sigma$ -phenyl protons, respectively. As expected, the two pyridine ring protons adjacent to the electronegative nitrogen atom, H<sup>2</sup> and H<sup>6</sup>, are shifted downfield compared to the other aromatic protons. Complex **8** has a very similar <sup>1</sup>H NMR spectrum to that of **5**, the main difference being the presence of a P-Me multiplet centered at  $\delta$  1.62, which constitutes the X part of an AMM'X<sub>3</sub>X<sub>3'</sub> spin system (where A = <sup>195</sup>Pt, M = <sup>31</sup>P, and X = <sup>1</sup>H).<sup>10–12</sup>

The isonicotinic acid complexes **6**, **9**, and **10** have the simplest <sup>1</sup>H NMR spectra because of their high symmetry. For example, **10** displays characteristic signals at  $\delta$  7.32, 6.87, and 7.05, assigned to the *ortho*, *meta*, and *para*  $\sigma$ -aryl protons, respectively. As anticipated, the aromatic region of the spectrum is significantly simplified without the presence

Scheme 1



of the PPh<sub>3</sub> proton signals. This aids in the assignment of the other aromatic protons that are masked by the PPh<sub>3</sub> protons in **5**, for example. The characteristic AA'XX' signals at  $\delta$  8.17 and 8.27 are attributed to the H<sup>2</sup> and H<sup>3</sup> protons of the isonicotinic acid ligand, respectively. As expected, the <sup>1</sup>H NMR spectra of the picolinic acid complexes **4** and **7** were more complicated than their respective isomers. For example, **7** shows a signal at  $\delta$  6.55 that is assigned to the *ortho*  $\sigma$ -aryl protons, and the multiplet signal at  $\delta$  6.87 is assigned to (overlapping) *meta* and *para*  $\sigma$ -aryl protons.

The <sup>31</sup>P{<sup>1</sup>H} NMR spectra of all complexes prepared in this work show a singlet flanked by <sup>195</sup>Pt satellite signals, consistent with mutually *trans* phosphine ligands. In contrast to PPh<sub>3</sub>, the presence of the electron-rich phosphine ligands PEt<sub>3</sub> and PMePh<sub>2</sub> leads to a significant upfield shift of the signal and a decrease in the magnitude of the <sup>195</sup>Pt-<sup>31</sup>P coupling constant.<sup>11</sup> The magnitudes of <sup>1</sup>J<sub>PtP</sub> for all complexes fall within the range that is typical for *trans*-substituted  $\sigma$ -arylplatinum(II) species.<sup>11,12</sup>

The IR spectra of **4–10** show the expected strong  $\nu$ (C=O) and broad  $\nu$ (O-H) bands at ca. 1720 cm<sup>-1</sup> and 2500–3200 cm<sup>-1</sup>, respectively, at frequencies that are typical for aromatic carboxylic acids.

### $pK_a$ Determinations

Potentiometric titration experiments were used to determine the  $pK_a$  value for the carboxylic acid functionality in complexes **6–10**.<sup>13</sup> All measurements were conducted in a 50% (v/v) EtOH/H<sub>2</sub>O solution at 295.0  $\pm$  0.1 K as the complexes were poorly soluble in water alone. Table 1

(13) The  $pK_a$  values of **4** and **5** could not be determined owing to their poor solubility in this solvent system.

- (8) (a) Aakeröy, C. B.; Beatty, A. M. *Chem. Commun.* **1998**, 1067. (b) Aakeröy, C. B.; Beatty, A. M.; Helfrich, B. A. *J. Chem. Soc., Dalton Trans.* **1998**, 1943.  
 (9) Gianneschi, N. C.; Tiekink, E. R. T.; Rendina, L. M. *J. Am. Chem. Soc.* **2000**, *122*, 8474.  
 (10) Crisp, M. G.; Pyke, S. M.; Rendina, L. M. *J. Organomet. Chem.* **2000**, *607*, 222.  
 (11) Pregosin, P. S.; Kunz, R. W. *<sup>31</sup>P and <sup>13</sup>C NMR of Transition Metal Complexes*; Springer: Berlin, 1979.  
 (12) Anderson, G. K.; Clark, H. C.; Davies, J. A. *Organometallics* **1982**, *1*, 64.

**Table 1.**  $pK_a$  Values for **6–10**<sup>a</sup>

complex	$pK_a$
<b>6</b>	$3.26 \pm 0.07$
<b>7</b>	$5.23 \pm 0.09$
<b>8</b>	$4.85 \pm 0.10$
<b>9</b>	$3.51 \pm 0.08$
<b>10</b>	$3.21 \pm 0.08$

<sup>a</sup> Measured in 50% (v/v) EtOH/H<sub>2</sub>O solution at  $295.0 \pm 0.1$  K.

summarizes the  $pK_a$  values that were determined for each of the complexes.

Comparisons between the acidities of the complexes prepared in this work and those of the free pyridine carboxylic acids are not pertinent in this context owing to the basic nature of the nitrogen atom present in the latter, which can act as an internal base and form the corresponding zwitterionic species. A more useful comparison of the acidities reported in Table 1 is with simple aromatic acids such as benzoic acid, the  $pK_a$  of which has been determined previously in 50% (v/v) EtOH/H<sub>2</sub>O solution ( $5.67 \pm 0.02$  at 298 K).<sup>14</sup> From the results presented in Table 1, it is clear that the complexes are significantly stronger Brønsted acids than benzoic acid, with **6** and **10** being approximately 300 times more acidic. This enhanced acidity is most likely attributed to the significant polarization of the O–H bond by the cationic platinum(II) center, thus promoting the facile loss of the acidic proton. The acidity of the complexes increases in the order **7**<sup>15</sup> < **8** < **9** < **6**  $\approx$  **10**, and it does not appear to be a function of the steric bulk or the basicity of the phosphine ligands; for example, the acidities of **6** and **10** are equal within experimental error, despite the obvious differences in the nature of the phosphine ligands. The acidities for the PMePh<sub>2</sub> series of complexes decrease in the order **7**<sup>15</sup> ( $R'' = 2\text{-CO}_2\text{H}$ ) < **8** ( $R'' = 3\text{-CO}_2\text{H}$ ) < **9** ( $R'' = 4\text{-CO}_2\text{H}$ ); that is, the acidities appear to follow the same order of the (estimated)  $pK_a$  values for free pyridine monocarboxylic acids with respect to the position of the CO<sub>2</sub>H group in the pyridine ring.<sup>16</sup>

Treatment of **6–10** with 1 equiv of base (e.g., KOH, KO<sup>t</sup>Bu, proton sponge) resulted in the isolation of mixtures containing the zwitterionic platinum(II) species and the corresponding triflate salt, for example, KOTf. Repeated attempts at purifying the zwitterionic triflate salt mixtures by repeated washings, recrystallization from numerous solvent systems, or column chromatography were unsuccessful. Only minor differences were found upon comparison of the NMR spectra of the pure cationic complexes with those of the corresponding zwitterions. For example, in the <sup>31</sup>P{<sup>1</sup>H} NMR spectrum of **9** and its corresponding zwitterion (in the presence of KOTf), the single resonance appears at  $\delta$  9.1 ( $^1J_{\text{PtP}} = 2883$  Hz) and  $\delta$  9.0 ( $^1J_{\text{PtP}} = 2894$  Hz), respectively,

(14) Niazi, M. S. K.; Mollin, J. *Bull. Chem. Soc. Jpn* **1987**, *60*, 2605.

(15) Caution should be exercised in the interpretation of  $pK_a$  phenomena involving **7** as it proved to be somewhat unstable in solution, particularly in the presence of polar solvents. This is most likely attributed to the considerable steric interactions between the 2-CO<sub>2</sub>H group and the PPh<sub>3</sub> ligands that, in addition to the strong *trans* effect exerted by the  $\sigma$ -phenyl ligand, would facilitate loss of the N-donor ligand.

(16) Green, R. W.; Tong, H. K. *J. Am. Chem. Soc.* **1956**, *78*, 4896.

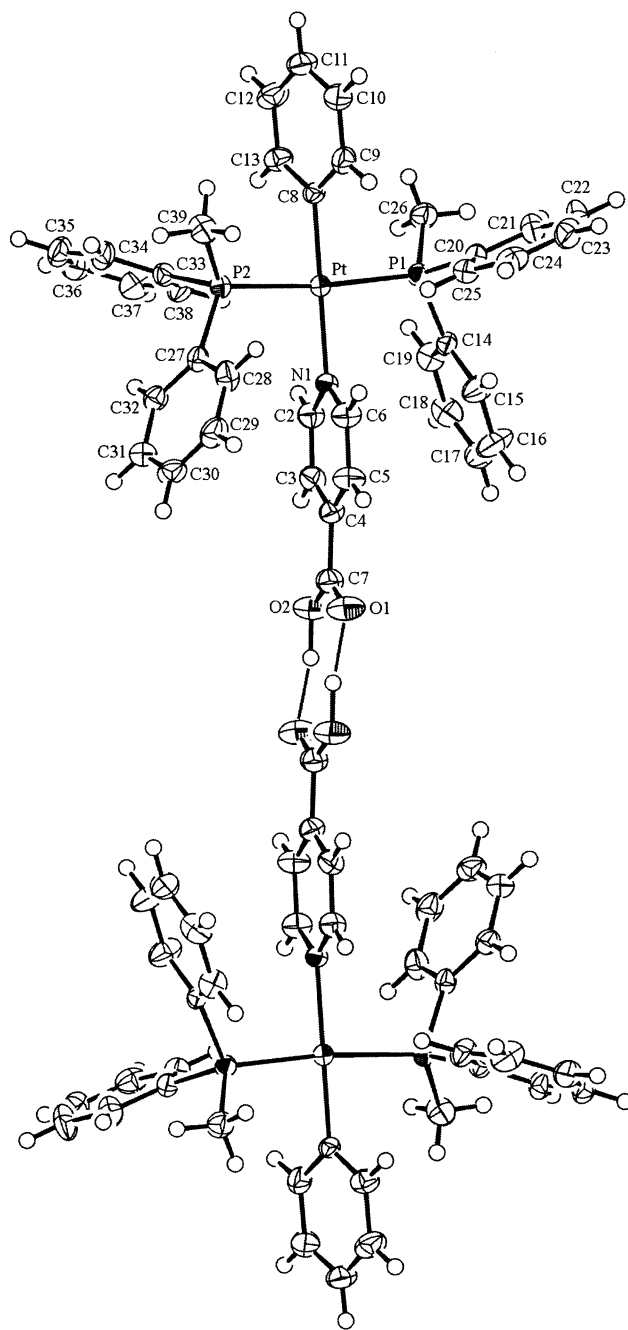


**Figure 1.** Molecular structure and crystallographic numbering scheme for **9**.

in 50% (v/v) EtOH/H<sub>2</sub>O solution. <sup>1</sup>H and <sup>31</sup>P{<sup>1</sup>H} NMR studies also confirmed the general robust nature of **6–10** and their corresponding zwitterionic species in various solvent systems, including that used in the  $pK_a$  experiments, even after prolonged periods of time (>100 h) at room temperature.

### X-ray Crystallography

The molecular structures of **9** and **10** are shown in Figures 1 and 2, respectively. Crystal data and refinement details are presented in Table 2, and selected geometric parameters are shown in Table 3. The asymmetric unit of each of **9** and **10** comprises a univalent complex cation, a triflate anion, and a solvent CH<sub>2</sub>Cl<sub>2</sub> molecule of crystallization. In each

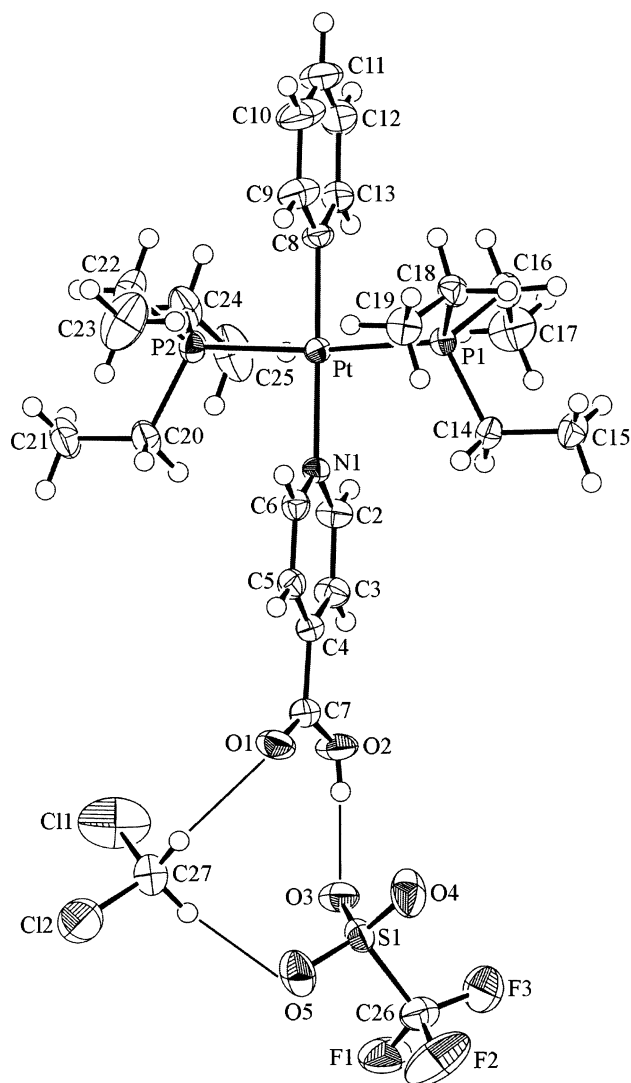


**Figure 2.** Molecular structure and crystallographic numbering scheme for **10**.

complex, the platinum atom exists in the expected square planar geometry defined by a C, N, P<sub>2</sub> donor set indicating that the isonicotinic acid is N-bound. The platinum atom lies 0.0102(1) and 0.0465(1) Å out of the respective coordination planes in **9** and **10**. In **10**, the platinum-bound phenyl and isonicotinic acid groups are effectively orthogonal to the square plane as seen in the magnitude of the dihedral angles of 88.6° and 89.4°, respectively. By contrast, in **9**, the respective dihedral angles are 74.5° and 91.5° with the large deviation for the phenyl group ascribed to the reduced steric hindrance imposed by the phosphine ligands on that side of the molecule. This result indicates that there is no preferential orientation for the platinum-bound phenyl group in **9** and **10**. While there are no significant differences in the geometric parameters defining the platinum atom interactions in the two structures (see Table 3), there is a fascinating difference in the mode of association between the molecules in the solid state.

As shown in Figure 1, centrosymmetrically related pairs of complex cations in **9** associate via the familiar carboxylic acid dimer motif. The details of this association are

**Table 2.** Crystallographic Data for **9** and **10**

	<b>9</b>	<b>10</b>
formula	C <sub>40</sub> H <sub>38</sub> Cl <sub>2</sub> F <sub>3</sub> NO <sub>5</sub> P <sub>2</sub> PtS	C <sub>26</sub> H <sub>42</sub> Cl <sub>2</sub> F <sub>3</sub> NO <sub>5</sub> P <sub>2</sub> PtS
fw	1029.7	865.6
cryst size, mm <sup>3</sup>	0.13 × 0.16 × 0.32	0.16 × 0.26 × 0.45
cryst syst	monoclinic	triclinic
space group	P2 <sub>1</sub> /n	P1̄
a, Å	11.367(3)	9.735(2)
b, Å	20.614(7)	10.839(4)
c, Å	17.583(5)	17.265(8)
α, deg	90	92.47(4)
β, deg	95.83(2)	94.93(3)
γ, deg	90	105.19(4)
V, Å <sup>3</sup>	4099(2)	1748(1)
Z	4	2
D <sub>calcd</sub> , g cm <sup>-3</sup>	1.669	1.645
F(000)	2040	860
μ, cm <sup>-1</sup>	37.27	43.52
no. data collected	10150	8439
θ <sub>max</sub> , deg	27.5	27.5
no. unique data	9679	8015
no. obsd data	6471	6714
with I ≥ 2.0σ(I)		
R, R <sub>w</sub> (obsd data)	0.030, 0.062	0.026, 0.061
R, R <sub>w</sub> (all data)	0.070, 0.072	0.042, 0.066
ρ <sub>max</sub> , e Å <sup>-3</sup>	0.95	0.90

**Table 3.** Selected Geometric Parameters (Å, deg) for **9** and **10**

	<b>9</b>	<b>10</b>
Pt–P1	2.3022(12)	2.3110(12)
Pt–P2	2.3080(12)	2.3095(13)
Pt–N1	2.134(3)	2.118(3)
Pt–C8	2.023(4)	2.027(4)
C7–O1	1.276(6)	1.193(5)
C7–O2	1.264(6)	1.323(5)
P1–Pt–P2	173.63(4)	174.38(4)
P1–Pt–N1	92.04(9)	93.31(9)
P1–Pt–C8	88.45(11)	86.92(12)
P2–Pt–N1	93.82(9)	92.29(9)
P2–Pt–C8	85.72(11)	87.50(12)
N1–Pt–C8	178.92(15)	178.91(16)

O2–H···O1<sup>i</sup> of 1.64 Å, O2···O1<sup>i</sup> of 2.709(5) Å, and an angle subtended at H of 171°; symmetry operation i:  $-x, 1 - y, 1 - z$ . The crystal structure also features significant interactions of the type C–H···π (Figure 3). The closest of these involves C17–H so that the distance between the H atom and the ring centroid of a translationally related C27–C32 phenyl ring is 2.72 Å; symmetry operation ii:  $-1 + x, y, z$ . The closest interaction involving the complex and triflate anion occurs between the phenyl C19–H and O3<sup>ii</sup> atoms so that H···O3<sup>ii</sup> is 2.48 Å and the angle at H is 139° (Figure 3). Finally, the shortest interaction involving the dichloromethane molecule involves the triflate so that C41–H is 2.30 Å from O5<sup>iii</sup> with an angle of 140° at H; symmetry operation iii:  $1 - x, 1 - y, -z$ . In contrast to that just described for **9**, the mode of intermolecular association in **10** is quite distinct.

Figure 2 shows the asymmetric unit for **10** and highlights the different types of intermolecular interactions operating in the crystal structure. Notable is the absence of the carboxylic acid dimer motif as found in **9**. Instead, the carboxylic acid residue forms both donor and acceptor interactions to the triflate anion and CH<sub>2</sub>Cl<sub>2</sub> solvent of crystallization, respectively, to afford a 10-membered ring structure. The details of the association between the carboxylic acid and triflate anion are O2–H···O3 of 1.88 Å,

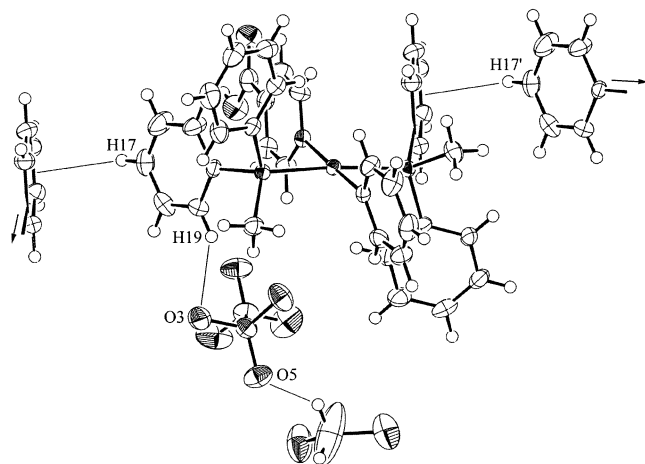


**Figure 3.** Diagram emphasizing the intermolecular associations formed by the complex cation **9** with the exception of the carboxylic acid dimer which is shown in Figure 1. Shown are the C—H $\cdots$  $\pi$ , involving the H17 atoms and the C27—C32 aromatic rings, and the C—H $\cdots$ O(triflate) contacts. Geometric parameters defining these associations are discussed in the text.

O2 $\cdots$ O3 of 2.665(4) Å, with an angle of 171° subtended at the H atom. For the interaction involving the dichloromethane molecule, C27—H $\cdots$ O1 is 2.40 Å, C27 $\cdots$ O1 is 3.244(7) Å, and angle at H is 143°. The second H atom of the dichloromethane molecule also forms a weak hydrogen bond, to O5 of the triflate, so that H $\cdots$ O5 is 2.47 Å, C27 $\cdots$ O5 is 3.196(6) Å, and the angle at H is 130°. While it is noted that the C—H $\cdots$ O interactions involving the dichloromethane molecule are not as well defined as are the O $\cdots$ H associations, such C—H $\cdots$ O are now well established in the literature.<sup>17</sup> The association between the molecules highlighted in Figure 2 has the result that a 10-membered ring is formed. As found for **9**, there are C—H $\cdots$  $\pi$  and C—H $\cdots$ O(triflate) interactions in the lattice of **10**. The distinct forms of intermolecular association involving the carboxylic acid groups in **9** and **10** gives rise to chemically important differences between the two sets of carboxylic acid C—O bond distances as may be noted from Table 3. In **9**, where strong intermolecular association resulting in carboxylic acid dimer formation has been observed, there is relatively little difference in the C—O bond distances; indeed, they are found to be equal within experimental error, a point emphasizing the strong nature of these contacts. By contrast, in **10**, where a relatively strong interaction was noted between the hydroxyl proton and the triflate anion and only a weak interaction between the carbonyl oxygen atom and the weakly acidic dichloromethane H-atom, there is a significant disparity in the C—O bond distances. This observation provides additional evidence that the “dichloromethane bridge” between the complex cation and triflate anion is only weak. Further, and consistent with this argument, is the systematic variation in the S—O bond distances such that the S1—O3 bond distance of 1.451(3) Å is significantly longer than the S1—O5 distance of 1.422(3) Å. It is interesting to speculate upon the reasons for the different crystal structures found for **9** and **10**.

In the context of the two structures reported herein, the absence of the carboxylic acid dimer motif in **10** is, perhaps,

unexpected. However, as has been mentioned in a recent review of hydrogen-bonding interactions operating in crystal structures of organic molecules,<sup>18</sup> the carboxylic acid dimer motif is not as pervasive as one might anticipate. Indeed, in this survey it was found that the classical dimer motif occurred in approximately one-third of the structures owing to the presence of competing hydrogen-bonding functionalities. This observation notwithstanding, it is curious that the carboxylic acid dimer motif is found in **9** but not in **10**. As mentioned already, the geometric parameters defining the two structures are essentially the same, and therefore, there does not appear to be an electronic reason to account for the disparate modes of association found in the solid state. In the same way, as has been noted in Table 1, the  $pK_a$  values of the carboxylic acid groups in the two complexes are similar, albeit these pertain to the solution phase. In the absence of any obvious chemical or structural imperatives, “subtle crystal packing effects” can be cited as the cause for the different crystal structures. Using an analogous argument cited for the appearance of polymorphs of tricyclohexylphosphinegold(I) 2-mercaptobenzoate, Au(SC<sub>6</sub>H<sub>4</sub>-2-CO<sub>2</sub>H)-PCy<sub>3</sub>, in which the carboxylic acid dimer motif was either present or not, it is possible to derive a qualitative explanation for these observations.<sup>19</sup> Basically, there are two considerations, namely, the formation of the carboxylic acid dimer motif with the concomitant formation of rod-shaped aggregates on one hand, and the absence of the dimer motif and the formation of balls or spherical aggregates on the other. Whereas the formation of the carboxylic dimer motif might be favorable in **10**, the consequence of this would be the formation of less favorable packing of rods, compared to the packing of spheres. Thus, in **9** the energy of stabilization in the lattice favors the formation of the carboxylic acid dimer motif and the global packing of the resultant rodlike entities. In **10**, the global packing considerations dominate so that rods are not formed.

## Conclusions

The considerable acidity of the CO<sub>2</sub>H functionality in complexes such as **6** and **10** may complicate host–guest studies involving these and related complexes, particularly when polar solvents are employed or traces of adventitious water are present in low polarity solvents. In the solid-state association of **9** and **10**, crystal packing effects appear to dictate the assembly of these complexes in the crystal lattice, and the expected carboxylic acid dimer motif is not necessarily observed. Even in the absence of such effects, the results of the X-ray study may have potential relevance to the molecular recognition properties of these and related cationic species in nonpolar solutions and, in certain cases, demonstrate that the counterion does not necessarily play a spectator role in the recognition process.

(17) Steiner, T. *Angew. Chem., Int. Ed.* **2002**, *41*, 48.

(18) Allen, F. H.; Motherwell, W. D. S.; Raithby, P. R.; Shields, G. P.; Taylor, R. *New J. Chem.* **1999**, 25.

(19) Smyth, D. R.; Vincent, B. R.; Tiekink, E. R. T. *Cryst. Growth Des.* **2001**, *1*, 113.

## Experimental Section

**General Methods.** All procedures were performed under an inert atmosphere of high purity N<sub>2</sub> using standard Schlenk techniques. CH<sub>2</sub>Cl<sub>2</sub> was distilled from CaH<sub>2</sub>. Toluene was predried over CaSO<sub>4</sub>, followed by distillation from sodium metal. Nicotinic, isonicotinic, and picolinic acids were obtained commercially (Aldrich) and were dried in a desiccator over P<sub>2</sub>O<sub>5</sub> prior to use. All 1D NMR spectra were recorded at 298 K by means of a Varian Gemini 2000 NMR spectrometer (<sup>1</sup>H at 300.10 MHz, <sup>19</sup>F at 282.23 MHz, and <sup>31</sup>P at 121.50 MHz). 2D COSY NMR spectroscopy experiments were performed on a Varian Unity INOVA 600 MHz NMR instrument. <sup>1</sup>H and <sup>19</sup>F{<sup>1</sup>H} chemical shifts are reported in ppm relative to TMS (0 ppm) and C<sub>6</sub>H<sub>5</sub>CF<sub>3</sub> (63.7 ppm), respectively. <sup>31</sup>P{<sup>1</sup>H} spectra were referenced to a sealed external standard of 85% H<sub>3</sub>PO<sub>4</sub> (0 ppm). IR spectra were recorded as Nujol mulls (NaCl plates) on a Perkin-Elmer Spectrum BX FT-IR spectrophotometer. Elemental analyses were determined by Chemical and Micro Analytical Services, Pty. Ltd., Victoria (Australia). *trans*-Iodophenylbis(triphenylphosphine)platinum(II) (**1**), *trans*-iodobis(methyldiphenylphosphine)phenylplatinum(II) (**2**), and *trans*-iodophenylbis(triethylphosphine)platinum(II) (**3**) were prepared from 1,5-cyclooctadiene(iodo)phenylplatinum(II) according to the general procedure outlined by Clark et al.<sup>12</sup>

***trans*-Phenyl(picolinic acid)bis(triphenylphosphine)platinum(II) triflate (**4**).** To a stirred solution of **1** (0.400 g, 0.433 mmol) in CH<sub>2</sub>Cl<sub>2</sub> (20 mL) was added AgOTf (0.106 g, 0.433 mmol). The mixture was stirred in the absence of light for 16 h, and AgI was removed by filtration through Celite filter aid. To the clear filtrate was added picolinic acid (0.0533 g, 0.433 mmol), and the mixture was stirred for 16 h at room temperature. The solvent was removed in vacuo to yield **4** as a white solid (0.270 g, 68%). IR (Nujol) 1720 ν(C=O), 2800–3100 ν(O–H) cm<sup>-1</sup>. <sup>1</sup>H NMR (CDCl<sub>3</sub>) δ 6.63 (d, 2H, <sup>3</sup>J<sub>HH</sub> = 7.5 Hz, H<sub>o</sub>), 6.33 (m, 2H, H<sub>m</sub>), 6.33 (m, 1H, H<sub>p</sub>), 8.69 (m, 1H, H<sup>3</sup>), 8.03 (d, 1H, <sup>3</sup>J<sub>HH</sub> = 7.8 Hz, H<sup>6</sup>), 8.28 (td, 1H, <sup>4</sup>J<sub>HH</sub> = 1.8 Hz, <sup>3</sup>J<sub>HH</sub> = 7.4 Hz, H<sup>5</sup>), 7.75 (m, 1H, H<sup>4</sup>), 7.52–7.14 (m, 30H, P–Ph). <sup>31</sup>P{<sup>1</sup>H} NMR δ 23.0 (s, <sup>1</sup>J<sub>PtP</sub> = 3212 Hz). Anal. Calcd for C<sub>25</sub>H<sub>40</sub>F<sub>3</sub>NO<sub>5</sub>P<sub>2</sub>PtS·CH<sub>2</sub>Cl<sub>2</sub>: C, 52.05; H, 3.67; N, 1.21. Found: C, 52.27; H, 3.86; N, 1.40.

***trans*-(Nicotinic acid)phenylbis(triphenylphosphine)platinum(II) Triflate (**5**).** Following a similar procedure to that described for **4**, complex **1** (0.300 g, 0.325 mmol) was treated with AgOTf (0.079 g, 0.309 mmol), followed by nicotinic acid (0.040 g, 0.325 mmol), to afford **5** as a white solid (0.312 g, 90%). IR (Nujol) 1720 ν(C=O), 2800–3200 ν(O–H) cm<sup>-1</sup>. <sup>1</sup>H NMR (CDCl<sub>3</sub>) δ 6.74 (d, 2H, <sup>3</sup>J<sub>HH</sub> = 7.5 Hz, H<sub>o</sub>), 6.37 (m, 2H, H<sub>m</sub>), 6.53 (m, 1H, H<sub>p</sub>), 8.57 (s, 1H, H<sub>2</sub>), 8.20 (d, 1H, <sup>3</sup>J<sub>HH</sub> = 5.7 Hz, H<sup>6</sup>), 6.82 (m, 1H, H<sup>5</sup>), 7.84 (d, 1H, <sup>3</sup>J<sub>HH</sub> = 7.8 Hz, H<sup>4</sup>), 7.57–7.14 (m, 30H, P–Ph). <sup>31</sup>P{<sup>1</sup>H} NMR δ 20.8 (s, <sup>1</sup>J<sub>PtP</sub> = 3045 Hz). <sup>19</sup>F NMR δ 48.4. Anal. Calcd for C<sub>49</sub>H<sub>40</sub>F<sub>3</sub>NO<sub>5</sub>P<sub>2</sub>PtS: C, 55.06; H, 3.77; N, 1.31. Found: C, 55.09; H, 3.78; N, 1.40.

***trans*-(Isonicotinic acid)phenylbis(triphenylphosphine)platinum(II) Triflate (**6**).** Following a similar procedure to that described for **4**, complex **1** (0.075 g, 0.081 mmol) was treated with AgOTf (0.019 g, 0.077 mmol), followed by isonicotinic acid (0.010 g, 0.081 mmol), to afford **6** as a white solid (0.078 g, 90%). IR (Nujol) 1726 ν(C=O), 2800–3100 ν(O–H) cm<sup>-1</sup>. <sup>1</sup>H NMR (CDCl<sub>3</sub>) δ 6.75 (d, 2H, <sup>3</sup>J<sub>HH</sub> = 6.9 Hz, <sup>3</sup>J<sub>PH</sub> = 24 Hz, H<sub>o</sub>), 6.31 (m, 2H, H<sub>m</sub>), 6.51 (m, 1H, H<sub>p</sub>), 8.35 (d, 2H, <sup>3</sup>J<sub>HH</sub> = 8.1 Hz, H<sup>6</sup>), 7.20 (m, 2H, H<sup>3/5</sup>), 7.43–7.27 (m, 30H, P–Ph). <sup>31</sup>P{<sup>1</sup>H} NMR δ 22.1 (s, <sup>1</sup>J<sub>PtP</sub> = 3054 Hz). Anal. Calcd for C<sub>49</sub>H<sub>40</sub>F<sub>3</sub>NO<sub>5</sub>P<sub>2</sub>PtS: C, 55.06; H, 3.77; N, 1.31. Found: C, 54.91; H, 3.73; N, 1.37.

***trans*-Phenyl(picolinic acid)bis(methyldiphenylphosphine)platinum(II) Triflate (**7**).** Following a similar procedure to that

described for **4**, complex **2** (0.400 g, 0.501 mmol) was treated with AgOTf (0.122 g, 0.501 mmol), followed by picolinic acid (0.062 g, 0.504 mmol), to afford **7** as a white solid (0.200 g, 58%). IR (Nujol) 1725 ν(C=O), 2700–3200 ν(O–H) cm<sup>-1</sup>. <sup>1</sup>H NMR (CDCl<sub>3</sub>) δ 6.55 (m, 2H, H<sub>o</sub>), 6.87 (m, 2H, H<sub>m</sub>), 6.87 (m, 1H, H<sub>p</sub>), 7.60 (m, 1H, H<sup>3</sup>), 8.68 (d, 1H, <sup>3</sup>J<sub>HH</sub> = 4.5 Hz, H<sup>6</sup>), 7.99 (td, 1H, <sup>3</sup>J<sub>HH</sub> = 7.4 Hz, <sup>4</sup>J<sub>HH</sub> = 1.8 Hz, H<sup>5</sup>), 8.25 (dt, 1H, <sup>3</sup>J<sub>HH</sub> = 7.50 Hz, <sup>4</sup>J<sub>HH</sub> = 1.2 Hz, H<sup>4</sup>), 7.42–7.18 (m, 20H, P–Ph), 1.42 (m, 6H, P–Me). <sup>31</sup>P{<sup>1</sup>H} NMR δ 6.5 (s, <sup>1</sup>J<sub>PtP</sub> = 3089 Hz). Anal. Calcd for C<sub>25</sub>H<sub>40</sub>F<sub>3</sub>NO<sub>5</sub>P<sub>2</sub>PtS: C, 49.58; H, 3.84; N, 1.48. Found: C, 49.53; H, 3.63; N, 1.59.

***trans*-Bis(methyldiphenylphosphine)(nicotinic acid)phenylplatinum(II) Triflate (**8**).** Following a similar procedure to that described for **4**, complex **2** (0.348 g, 0.436 mmol) was treated with AgOTf (0.106 g, 0.414 mmol), followed by nicotinic acid (0.0537 g, 0.436 mmol), to afford **8** as a white solid (0.312 g, 88%). IR (Nujol) 1720 ν(C=O), 2800–3200 ν(O–H) cm<sup>-1</sup>. <sup>1</sup>H NMR (CDCl<sub>3</sub>) δ 8.37 (s, 1H, H<sup>2</sup>), 8.19 (d, 1H, <sup>3</sup>J<sub>HH</sub> = 4.8 Hz, H<sup>6</sup>), 6.89 (m, 1H, H<sup>5</sup>), 7.88 (d, 1H, <sup>3</sup>J<sub>HH</sub> = 8.1 Hz, H<sup>4</sup>), 7.52–7.16 (m, 20H, P–Ph), 1.62 (m, 6H, P–Me). <sup>31</sup>P{<sup>1</sup>H} NMR δ 9.4 (s, <sup>1</sup>J<sub>PtP</sub> = 2870 Hz). <sup>19</sup>F NMR δ 48.5. Anal. Calcd for C<sub>39</sub>H<sub>36</sub>F<sub>3</sub>NO<sub>5</sub>P<sub>2</sub>PtS: C, 49.58; H, 3.84; N, 1.48. Found: C, 49.60; H, 3.74; N, 1.53.

***trans*-Bis(methyldiphenylphosphine)(isonicotinic acid)phenylplatinum(II) Triflate (**9**).** Following a similar procedure to that described for **4**, complex **2** (0.132 g, 0.165 mmol) was treated with AgOTf (0.040 g, 0.157 mmol), followed by isonicotinic acid (0.020 g, 0.162 mmol), to afford **9** as a white solid (0.132 g, 85%). IR (Nujol) 1712 ν(C=O), 2500–3000 ν(O–H) cm<sup>-1</sup>. <sup>1</sup>H NMR (CDCl<sub>3</sub>) δ 8.17 (d, 2H, <sup>3</sup>J<sub>HH</sub> = 6.6 Hz, H<sup>2/6</sup>), 6.78 (m, 2H, H<sup>3/5</sup>), 7.45–7.23 (m, 20H, P–Ph), 1.64 (m, 6H, P–Me). <sup>31</sup>P{<sup>1</sup>H} NMR δ 9.4 (s, <sup>1</sup>J<sub>PtP</sub> = 2914 Hz). <sup>19</sup>F NMR δ 48.5. Anal. Calcd for C<sub>39</sub>H<sub>36</sub>F<sub>3</sub>NO<sub>5</sub>P<sub>2</sub>PtS: C, 49.58; H, 3.84; N, 1.48. Found: C, 49.44; H, 3.88; N, 1.42.

***trans*-(Isonicotinic acid)phenylbis(triethylphosphine)platinum(II) Triflate (**10**).** Following a similar procedure to that described for **4**, complex **3** (0.255 g, 0.402 mmol) was treated with AgOTf (0.098 g, 0.381 mmol), followed by isonicotinic acid (0.049 g, 0.402 mmol), to afford **10** as a white solid (0.298 g, 95%). IR (Nujol) 1731 ν(C=O), 2700–3100 ν(O–H) cm<sup>-1</sup>. <sup>1</sup>H NMR (CDCl<sub>3</sub>) δ 7.32 (d, 2H, <sup>3</sup>J<sub>HH</sub> = 8.1 Hz, <sup>3</sup>J<sub>PH</sub> = 29 Hz, H<sub>o</sub>), 6.87 (m, 2H, H<sub>m</sub>), 7.05 (m, 1H, H<sub>p</sub>), 8.89 (d, 2H, <sup>3</sup>J<sub>HH</sub> = 6.3 Hz, H<sup>2/6</sup>), 8.27 (m, 2H, <sup>3</sup>J<sub>HH</sub> = 6.6 Hz, H<sup>3/5</sup>), 1.73–1.02 (m, 30H, PEt<sub>3</sub>). <sup>31</sup>P{<sup>1</sup>H} NMR δ 13.4 (s, <sup>1</sup>J<sub>PtP</sub> = 2697 Hz). <sup>19</sup>F NMR δ 48.2. Anal. Calcd for C<sub>25</sub>H<sub>40</sub>F<sub>3</sub>NO<sub>5</sub>P<sub>2</sub>PtS: C, 38.46; H, 5.16; N, 1.79. Found: C, 38.46; H, 5.15; N, 1.72.

**Determination of pK<sub>a</sub> Values.** pK<sub>a</sub> determinations were carried out in triplicate by preparing a stock solution (0.01 mol dm<sup>-3</sup>) of the complex of interest in degassed 50% (v/v) EtOH/H<sub>2</sub>O solution. The solution was then titrated with KOH solution (0.1 mol dm<sup>-3</sup>) prepared in the same solvent system. The pH of the solution was measured using a calibrated glass electrode with a 0.1 mol dm<sup>-3</sup> silver–silver chloride electrode at 295.0 ± 0.1 K. The pK<sub>a</sub> value for each of the complexes was calculated by means of the procedure reported by Albert and Serjeant.<sup>20</sup>

**X-ray Diffraction.** Suitable colorless crystals of **9** and **10** were grown from CH<sub>2</sub>Cl<sub>2</sub>/*n*-hexane by means of diffusion-layering techniques. Data for the crystals were collected at 173 K employing graphite monochromatized Mo Kα radiation, λ = 0.71069 Å, on a Rigaku AFC7R diffractometer. Corrections were made for Lorentz

(20) Albert, A.; Serjeant, E. P. *The Determination of Ionization Constants: A Laboratory Manual*, 3rd ed.; Chapman and Hall: New York, 1984.

and polarization effects,<sup>21</sup> and for absorption using an empirical procedure (DIFABS<sup>22</sup>). Crystal data and refinement details are given in Table 2.

The structures were solved by heavy-atom methods,<sup>23</sup> and each was refined by a full-matrix least-squares procedure based on  $F^2$ .<sup>21</sup> Non-hydrogen atoms were refined with anisotropic displacement parameters, and hydrogen atoms were included in the model in their calculated positions; the O–H atom was located from a difference map in each case. The refinements were continued until convergence after the application of a weighting scheme of the form  $w = 1/[\sigma^2(F_o)^2 + (0.0243P)^2 + 2.1531P]$  for **9** and  $w = 1/[\sigma^2(F_o)^2 + (0.0239P)^2 + 2.7679P]$  for **10**, where  $P = (F_o^2 + 2F_c^2)/3$ . The numbering schemes, shown in Figures 1–3, were drawn with ORTEP<sup>24</sup> at 50% displacement ellipsoids.

(21) *teXsan: Structure Analysis Software*; Molecular Structure Corp.: The Woodlands, TX, 1997.

(22) Walker, N.; Stuart, D. *Acta Crystallogr., Sect. A* **1983**, *39*, 158.

**Acknowledgment.** We thank Mr P. Clements for recording the COSY NMR spectra, and Dr S. M. Pyke for useful NMR discussions. We also thank Johnson Matthey for the generous loan of  $K_2[PtCl_4]$ . We are grateful to the Australian Research Council (ARC) and the University of Adelaide for financial support.

**Supporting Information Available:** X-ray crystallographic data files for **9** and **10**, including atomic coordinates, bond distances and angles, and thermal parameters, in CIF format. This material is available free of charge via the Internet at <http://pubs.acs.org>.

IC025776A

(23) Beurskens, P. T.; Admiraal, G.; Beurskens, G.; Bosman, W. P.; García-Granda, S.; Smits, J. M. M.; Smykalla, C. *The DIRDIF Program System*; Technical Report of the Crystallography Laboratory; The University of Nijmegen: Nijmegen, The Netherlands, 1992.

(24) Johnson, C. K. *ORTEP*; Report ORNL-5138; Oak Ridge National Laboratory, TN, 1976.